

# Nonvisual Arrestins Function as Simple Scaffolds Assembling the MKK4–JNK3 $\alpha$ 2 Signaling Complex

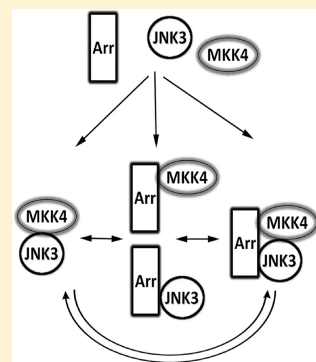
Xuanzhi Zhan,<sup>†</sup> Tamer S. Kaoud,<sup>‡</sup> Kevin N. Dalby,<sup>‡</sup> and Vsevolod V. Gurevich<sup>\*,†</sup>

<sup>†</sup>Department of Pharmacology, Vanderbilt University, Nashville, Tennessee 37232, United States

<sup>‡</sup>Division of Medicinal Chemistry, The University of Texas at Austin, Austin, Texas 78712, United States

## Supporting Information

**ABSTRACT:** Arrestins make up a small family of proteins with four mammalian members that play key roles in the regulation of multiple G protein-coupled receptor-dependent and -independent signaling pathways. Although arrestins were reported to serve as scaffolds for MAP kinase cascades, promoting the activation of JNK3, ERK1/2, and p38, the molecular mechanisms involved were not elucidated, and even the direct binding of arrestins with MAP kinases was never demonstrated. Here, using purified proteins, we show that both nonvisual arrestins directly bind JNK3 $\alpha$ 2 and its upstream activator MKK4, and that the affinity of arrestin-3 for these kinases is higher than that of arrestin-2. Reconstitution of the MKK4–JNK3 $\alpha$ 2 signaling module from pure proteins in the presence of different arrestin-3 concentrations showed that arrestin-3 acts as a “true” scaffold, facilitating JNK3 $\alpha$ 2 phosphorylation by bringing the two kinases together. Both the level of JNK3 $\alpha$ 2 phosphorylation by MKK4 and JNK3 $\alpha$ 2 activity toward its substrate ATF2 increase at low and then decrease at high arrestin-3 levels, yielding a bell-shaped concentration dependence expected with true scaffolds that do not activate the upstream kinase or its substrate. Thus, direct binding of both kinases and true scaffolding is the molecular mechanism of action of arrestin-3 on the MKK4–JNK3 $\alpha$ 2 signaling module.



Arrestins were first discovered as negative regulators of G protein-coupled receptor (GPCR) signaling (reviewed in refs 1 and 2). Arrestins bind to the cytoplasmic side of active receptors phosphorylated by GRKs, blocking further G protein coupling by steric exclusion.<sup>3,4</sup> Nonvisual arrestin-2<sup>a</sup> and -3 facilitate recruitment of the GPCR to the coated pit by virtue of direct interactions of the arrestin C-tail with clathrin<sup>5</sup> and adaptor AP2.<sup>6</sup> Recent studies revealed a second, G protein-independent round of signaling initiated by the receptor-bound arrestins via interactions with a variety of nonreceptor partners (reviewed in refs 7 and 8). In particular, the arrestin–receptor complex was reported to act as a scaffold for three mitogen-activated protein kinase (MAPK) cascades, leading to the activation of JNK3,<sup>9</sup> ERK1/2,<sup>10</sup> and p38.<sup>11</sup> While initial work suggested that only the arrestin–receptor complex serves as the initiator of signaling,<sup>9–11</sup> subsequent studies demonstrated that free arrestins interact with many of the same proteins<sup>12–18</sup> and appear to promote JNK3 $\alpha$ 2 activation in a manner independent of GPCRs.<sup>15,18,19</sup>

MAPKs regulate critical cellular signaling pathways involved in cell proliferation, motility, differentiation, and apoptosis.<sup>20</sup> The core of all MAPK signaling modules conserved throughout eukaryotes comprises the three-kinase cascade, where MAP kinase kinase kinase (MAP3K) activates by phosphorylation MAP kinase kinase (MAP2K), whereupon it phosphorylates MAPK, which then phosphorylates different substrates.<sup>21,22</sup> Signal transduction in MAPK cascades is usually regulated by scaffolding proteins that assemble these kinases into signaling complexes. By tethering the kinase components into a

multienzyme complex, the scaffolds provide an insulated physical conduit through which signals can be amplified and transmitted to the appropriate spatiotemporal cellular loci. Despite identification of new scaffold proteins and probing of their functional roles, the molecular mechanisms of scaffolding remain unclear.

Using purified arrestin-2, arrestin-3, JNK3 $\alpha$ 2, and upstream MAP2K MKK4 here, we demonstrated for the first time the direct interaction of JNK3 $\alpha$ 2 and MKK4 with both nonvisual arrestins. By reconstruction of the arrestin–MKK4–JNK3 $\alpha$ 2 signaling module in vitro, we show that arrestins act as true scaffolds, bringing JNK3 $\alpha$ 2 and its activator, MKK4, together. Consistent with true scaffolding, the dependence of the JNK3 $\alpha$ 2 activation by MKK4 on arrestin-3 concentration is biphasic: an increase at lower levels is followed by a decrease at high arrestin-3 concentrations. Kinetic analysis of JNK3 $\alpha$ 2 phosphorylation by MKK4 in the presence of different arrestin-3 concentrations also shows that the time course of JNK3 $\alpha$ 2 activation is significantly affected by scaffold concentration. This is the first experimental evidence demonstrating these theoretically predicted phenomena.<sup>23,24</sup>

**Received:** September 27, 2011

**Revised:** October 29, 2011

**Published:** November 2, 2011



## MATERIALS AND METHODS

**Materials.** All restriction enzymes were from New England Biolabs. Other chemicals were from sources previously described.<sup>25,26</sup>

**Protein Purification.** Wild-type (WT) and mutant arrestin-2 and arrestin-3 proteins were purified, as previously described.<sup>27,28</sup> Briefly, untagged bovine arrestins were expressed in *Escherichia coli* and purified by sequential Heparin-Sepharose and Q-Sepharose chromatography to >95% purity, as judged by Coomassie blue staining. Two versions of His-tagged JNK2 $\alpha$ 2 with the same activity were used. In one, human JNK3 $\alpha$ 2 cDNA was subcloned into the pTrc-His2 vector between NcoI and BamHI sites, so that the His<sub>6</sub> tag was added at the C-terminus. In the other, JNK2 $\alpha$ 2 was His-tagged at the N-terminus, and the tag was cleaved off after purification. *E. coli* strain BL21(DE3) was used for expression. The cells were grown in LB to an A<sub>600</sub> of 0.4–0.8 and then induced with 0.1 mM isopropyl  $\beta$ -D-thiogalactoside at 22 °C for 5–6 h. The cells from 6 L of culture were pelleted by centrifugation, resuspended in buffer containing 10 mM imidazole, 100 mM NaCl, and 20 mM Tris-HCl (pH 7.5), and lysed by being frozen and thawed in the presence of lysozyme (3 mg/L), followed by sonication (3  $\times$  15 s). After centrifugation (9000 rpm for 90 min, Sorvall SLA-3000 rotor), the supernatants were passed through a 5 mL nickel-NTA (Qiagen) chromatographic column. The column was washed with 50 mL of buffer containing 50 mM imidazole, 100 mM NaCl, and 20 mM Tris-HCl (pH 7.5). The proteins were eluted with 50 mL of the same buffer containing 250 mM imidazole. After the NaCl concentration had been adjusted to 500 mM, the eluate was loaded onto a 15 mL phenyl-Sepharose column and eluted with a 300 mL gradient from 0 to 70% ethylene glycol. Fractions containing JNK3 $\alpha$ 2 (50–80 mL) were diluted 10-fold with 5 mM Tris-HCl (pH 7.5) and loaded onto a 10 mL SP-Sepharose column. JNK3 $\alpha$ 2 was eluted with a 300 mL gradient from 0 to 300 mM NaCl in 20 mM Tris-HCl (pH 7.5) buffer. Fractions containing JNK3 $\alpha$ 2 (>95% pure) were pooled, concentrated to ~1 mg/mL, and stored at –80 °C.

**Construction of pGEX4T1-MKK4.** A construct encoding full-length wild-type human mitogen-activated protein kinase kinase 4 (MAP2K4) (GenBank accession number NM\_003010) with an N-terminal cleavable GST tag was created by polymerase chain reaction (PCR) amplification of an MKK4 template by using the following oligonucleotides: forward (5'-CGT **GGA TCC ATG GCG GCT CCG AGC CCG AGC GGC GGC**-3') (BamHI site in bold) and reverse (5'-CCG **CTC GAG TTA TCA ATC GAC ATA CAT GGG AGA GCT GGG AGT**-3') (XhoI site in bold). The PCR product was digested with BamHI and XhoI and then ligated into a BamHI- and XhoI-digested pGEX-4T1 vector. After transformation of the ligation mixture into DH5 $\alpha$  *E. coli* cells with the appropriate antibiotic, the correct construct was recovered using standard molecular biology procedures. The sequence was verified at the Institute for Cell and Molecular Biology (ICMB) Sequencing Facility at The University of Texas at Austin.

**Expression and Purification of GST-MKK4.** The pGEX4T1-MKK4 vector was transformed into BL21(DE3) electrocompetent cells. A single colony of freshly transformed cells was inoculated in a 30 mL culture of Luria broth (LB) containing 50  $\mu$ g/mL ampicillin and then incubated while being shaken overnight at 37 °C. The culture was diluted 100-fold

into TB (Terrific Broth) medium containing 50  $\mu$ g/mL ampicillin and incubated with shaking at 37 °C until the OD<sub>600</sub> reached 0.6–0.7. GST-MKK4 expression was induced by 25–50  $\mu$ M IPTG, and shaking continued at 25 °C for 20 h. The cells were pelleted (8000g for 15 min), immediately frozen in liquid nitrogen, and stored at –80 °C. Frozen wet cells were resuspended in 150 mL of buffer A [10 mM Na<sub>2</sub>HPO<sub>4</sub>, 1.8 mM KH<sub>2</sub>PO<sub>4</sub> (pH 7.3), 140 mM NaCl, 2.7 mM KCl, 0.1% 2-mercaptoethanol, 0.1 mM TPCK, 0.1 mM PMSF, and 1 mM benzamidine] containing 0.2 mg/mL lysozyme, 1 mM MgCl<sub>2</sub>, and 20% (v/v) glycerol. The mixture was incubated at 4 °C for 30 min, and then Triton X-100 was added to a final concentration of 1% (v/v) and the incubation at 4 °C extended for an additional 30 min. The cell lysate was sonicated at 4 °C for 5–10 min (5 s pulses with 5 s intervals and careful monitoring of the temperature using a temperature probe). The lysate was then centrifuged for 30 min at 12000g and the supernatant mixed with 10 mL of Glutathione Sepharose High Performance (Amersham Biosciences) equilibrated in buffer A and shaken gently for 1.5 h at 4 °C. The beads were washed with 150 mL of buffer A. The GST-tagged proteins were eluted with 20 mL of buffer B [50 mM Tris-HCl (pH 7.5) containing 20 mM reduced glutathione, 0.1% 2-mercaptoethanol, 0.1 mM TPCK, 0.1 mM PMSF, 1 mM benzamidine, and 20% (v/v) glycerol]. The eluted protein was collected and dialyzed into buffer S [25 mM Hepes (pH 7.5), 50 mM KCl, 0.1 mM EDTA, 0.1 mM EGTA, and 2 mM DTT] containing 20% glycerol. The protein was measured using Bradford reagent. The estimated yield was around 20–30 mg of pure GST-MKK4/L of cells.

**Activation of GST-MKK4.** GST-MKK4 (4  $\mu$ M) and GST-MEKK1c (2  $\mu$ M) (320 C-terminal amino acids corresponding to the catalytic domain) were incubated at 30 °C for 60 min in the presence of 4 mM ATP in 10 mL of activation buffer C [25 mM Hepes (pH 7.5), 20 mM MgCl<sub>2</sub>, 0.1 mM EDTA, 0.1 mM EGTA, and 2 mM dithiothreitol] and repurified using a gel filtration column (120 mL HiLoad 16/60 Superdex 200 prep grade column) that had been equilibrated with 25 mM Hepes buffer (pH 7.5) containing 100 mM KCl, 0.1 mM EDTA, 0.1 mM EGTA, and 2 mM TCEP. This column purifies the active GST-MKK4 from the constitutively active GST-MEKK1c. The activated GST-MKK4 was stored in buffer S containing 20% glycerol at –80 °C until further use. At least 65% of GST-MKK4 was recovered as pure active GST-MKK4.

**His Tag Pull-Down Assay.** Binding of arrestin-2 and -3 to His-tagged JNK3 $\alpha$ 2 was assayed by the His tag pull-down assay of the complex with Ni-NTA resin (Qiagen), according to the manufacturer's instructions. Briefly, 25  $\mu$ L of purified JNK3 $\alpha$ 2-His (20  $\mu$ g) and 1 mM BSA were incubated with 25  $\mu$ L of Ni-NTA resin (50% slurry) in binding buffer [50 mM Hepes (pH 7.3) and 150 mM NaCl] at 4 °C with gentle rotation for 2 h. Subsequently, 50  $\mu$ L of a solution containing 10  $\mu$ g of arrestin, 1 mM BSA, and 50 mM imidazole was added to a suspension of Ni-NTA and JNK3 $\alpha$ 2 and incubated at 4 °C with gentle rotation for 2 h. The suspension was transferred to centrifuge filters (Ultrafree, Millipore) and washed three times with 200  $\mu$ L of wash buffer [50 mM imidazole, 50 mM Hepes (pH 7.3), and 150 mM NaCl]. The proteins were eluted from the Ni-NTA beads by the addition of 100  $\mu$ L of elution buffer [250 mM imidazole, 50 mM Hepes (pH 7.3), and 150 mM NaCl]. The eluates were analyzed by sodium dodecyl sulfate–polyacrylamide gel electrophoresis (SDS–PAGE) and Western blotting. Samples obtained in the absence of JNK3 $\alpha$ 2-His served as controls for nonspecific binding.

**GST Pull-Down Assay.** The GST pull-down assay was used to analyze the binding of arrestin-2 and -3 to MKK4. Purified GST-MKK4 (25  $\mu$ L, 10  $\mu$ g) was incubated with 25  $\mu$ L of glutathione-agarose resin (50% slurry, Sigma) in binding buffer [50 mM Hepes (pH 7.3) and 150 mM NaCl] at 4 °C with gentle rotation for 2 h. Arrestin (20  $\mu$ L, 10  $\mu$ g) was added, and the suspensions were incubated with rotation at 4 °C for 2 h. The suspensions were transferred to centrifuge filters and washed three times with 300  $\mu$ L of binding buffer. The proteins were eluted from resin by the addition of 100  $\mu$ L of elution buffer [100 mM glutathione, 50 mM Hepes (pH 7.3), and 150 mM NaCl]. Eluates were analyzed by SDS–PAGE and Western blotting. Samples obtained with GST bound to the column served as controls for nonspecific binding.

**Fluorescence Resonance Energy Transfer (FRET) Assay.** The binding affinities of both nonvisual arrestins for JNK3 were determined using a FRET assay. Single-cysteine mutants of arrestin-2 and -3 (arrestin-2-S234C and arrestin-3-L101C, respectively) generated on the background of fully active cysteine-less mutants<sup>25</sup> were labeled with fluorescein-5-maleimide (Thermo Scientific), and wild-type JNK3 $\alpha$ 2 was labeled with Alexa Fluor 568 C<sub>5</sub> Maleimide (Invitrogen), according to the manufacturers' protocols with minor modifications. The binding of proteins labeled with fluorescent probes was evaluated using a His tag pull-down assay. FRET between donor fluorescein-labeled arrestins (50 nM) and acceptor Alexa 568-labeled JNK3 (0–10  $\mu$ M) was assessed in a spectrofluorometer (Photon Technology International). Fluorescence emission spectra were recorded at 25 °C with excitation at 485 nm. Donor and acceptor only samples displayed distinct emission maxima at 518 and 600 nm, respectively (Figure S1 of the Supporting Information). The dissociation constants were calculated on the basis of the decrease in the magnitude of the donor signal. The data were fitted to the one-site binding equation using GraphPad Prism 4.

**Activation of JNK3 $\alpha$ 2 by MKK4 Assessed via an in Vitro Kinase Activity Assay.** The effect of arrestins on the phosphorylation of JNK3 $\alpha$ 2 by MKK4 was analyzed by an in vitro MKK4 kinase activity assay. The assays were conducted in 10  $\mu$ L containing the following final concentrations: 10 mM Hepes-Na (pH 7.3), 100 mM NaCl, 5 mM MgCl<sub>2</sub>, 2 mM DTT, 50 nM active MKK4, 0.5  $\mu$ M JNK3 $\alpha$ 2, and 0–30  $\mu$ M arrestin-3. The reactions were initiated by the addition of 0.2 mM ATP (4  $\mu$ Ci of  $\gamma$ -<sup>32</sup>P) and the mixtures incubated individually at 30 °C for the indicated time. The reactions were stopped by the addition of 15  $\mu$ L of Laemmli SDS sample buffer (Sigma) and the mixtures subjected to PAGE (10%). The gels were stained with Coomassie blue and dried. Phosphorylated JNK3 $\alpha$ 2 was visualized by autoradiography. The bands were cut out, and the radioactivity was measured in a Tri-Carb liquid scintillation counter (PerkinElmer).

**Phosphorylation of ATF2 by JNK3 $\alpha$ 2.** The enzymatic activity of JNK3 $\alpha$ 2 in the presence of MKK4 with or without arrestin-3 was determined by measuring the phosphorylation of the JNK3 $\alpha$ 2 substrate ATF2. The reactions were conducted in 10  $\mu$ L containing 10 mM Hepes-Na (pH 7.3), 100 mM NaCl, 10 mM MgCl<sub>2</sub>, 2 mM DTT, 50 nM active MKK4, 1  $\mu$ M inactive JNK3 $\alpha$ 2, and 0–30  $\mu$ M arrestin-3. The reactions were initiated by the addition of 0.3 mM ATP. After 4 min, 7  $\mu$ L of the reaction mixture was transferred to another reaction mixture containing 20  $\mu$ M purified GST-ATF2 (1–115) and 0.3 mM radiolabeled [ $\gamma$ -<sup>32</sup>P]ATP (specific activity of  $1 \times 10^{15}$  cpm/mol) in a final volume of 70  $\mu$ L. The reaction mixture was

incubated at 30 °C. Aliquots (10  $\mu$ L) were spotted onto P81 filter paper at different times (0.5, 1, 1.5, 2, and 4 min). The filter paper was washed three times for 15 min with 50 mM phosphoric acid to remove excess ATP and then once with acetone for drying. The amount of phosphate incorporated into ATF2 was determined by scintillation counting (Packard 1500).

## RESULTS

**MKK4 Directly Binds Arrestin-2 and -3 with Different Affinities.** Previous studies reported a weak association between MKK4 and arrestin-3, and this binding was enhanced in the presence of JNK3 and ASK1.<sup>9</sup> Recently, we found that all four arrestins co-immunoprecipitate (co-IP) MKK4.<sup>15</sup> However, it remained unclear whether MKK4 binds arrestins directly or indirectly, as all previous studies used co-IP from cell lysates, where the interaction could have been mediated by any of the hundreds of other proteins present. To resolve this issue, we performed a GST pull-down assay to detect the binding between MKK4 and arrestin-2 and -3 using purified proteins (Figure 1A), with an equal amount of GST serving as a negative

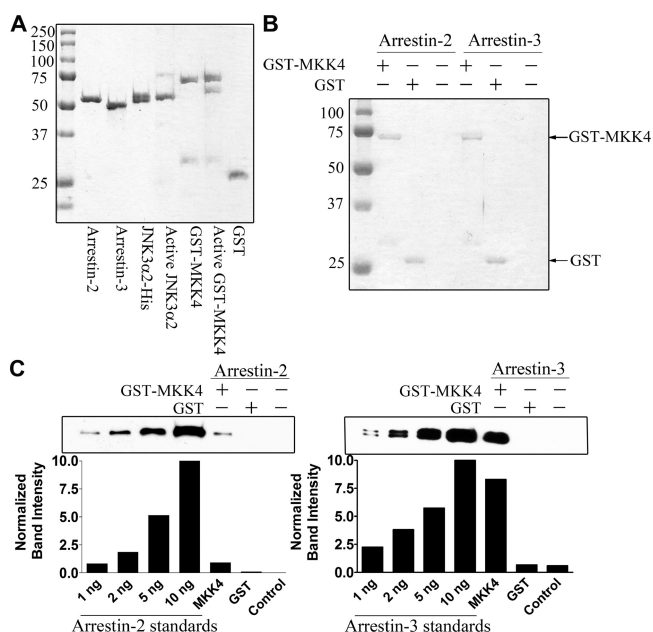


**Figure 1.** Nonvisual arrestins directly bind MKK4 with different affinities. (A) Coomassie blue-stained SDS–PAGE gel showing the purity of the indicated proteins used in this study. (B) Coomassie blue staining of GST and GST-MKK4 eluted from the glutathione column, showing equal loading. (C) The results of the GST pull-down assay showed that both nonvisual arrestins are retained by GST-MKK4, but not by the GST column. Western blots of the eluates from indicated columns (one-fifth loaded); lanes containing known amounts of purified arrestin-2 and -3 were used as standards to generate calibration curves. Quantification shows that GST-MKK4 column retained  $0.8 \pm 0.3$  and  $7.5 \pm 2.4$  ng of arrestin-2 and -3, respectively. The results of a representative experiment out of three performed are shown.

control (Figure 1B). We found that MKK4 directly binds both nonvisual arrestins. The binding to arrestin-3 was tighter than to arrestin-2, as judged by the presence of  $\sim 7.5 \pm 2.4$  ng of arrestin-3 and  $0.8 \pm 0.3$  ng of arrestin-2 in one-fifth of the eluted samples (Figure 1C). No nonspecific binding to GST



was detected. These data provide the first experimental evidence that MKK4 directly interacts with nonvisual arrestins.

Stronger binding to arrestin-3 than to arrestin-2 was a surprising finding, because co-IP studies suggested that both nonvisual arrestins bind MKK4 similarly.<sup>15</sup> However, the association of MKK4 with arrestins detected by co-IP was weak and may not have been sensitive enough to reveal different affinities of the two nonvisual arrestins. The level of co-IP was also affected by the presence of the other kinases of this module, ASK1 and JNK3.<sup>15</sup> In contrast, the pull-down assay with purified proteins detects only the direct binding between arrestins and MKK4 in precisely controlled conditions, making this assay more reliable. Stronger binding of arrestin-3 to MKK4 is consistent with an earlier demonstration that arrestin-3 is the only isoform that enhances JNK3 $\alpha$ 2 phosphorylation in COS-7 cells,<sup>9,15,19</sup> although all arrestins bind all kinases in the ASK1–MKK4–JNK3 cascade.<sup>14,15,18,29</sup>

**Arrestin-2 and -3 Directly Bind JNK3 $\alpha$ 2 with Comparable Affinity.** The association with JNK3 $\alpha$ 2 was the first interaction between arrestins and MAP kinases described.<sup>9</sup> The original study suggested that only arrestin-3 interacts with JNK3 $\alpha$ 2, and later a putative motif in the C-domain of arrestin-3, absent in arrestin-2, was tentatively identified as the JNK3 $\alpha$ 2 binding site.<sup>19</sup> This motif turned out to be specific for rodent arrestin-3,<sup>1</sup> and subsequent studies showed that all arrestins interact with JNK3 $\alpha$ 2 and move it out of the nucleus to the cytoplasm.<sup>12–15,29</sup> JNK3 $\alpha$ 2 was also shown to bind comparably to WT arrestins, as well as “pre-activated” mutants and arrestins “frozen” in the basal conformation.<sup>14,29</sup> However, previous analysis of the interaction between JNK3 and arrestins was performed in cells, leaving open the possibility that this interaction is indirect, mediated by other cellular proteins.

To investigate whether the binding between JNK3 $\alpha$ 2 and nonvisual arrestins is direct, we used purified arrestins and JNK3 $\alpha$ 2-His in an in vitro His tag pull-down assay (Figure 2A–C). We found that both arrestin-2 and -3 directly associate with JNK3 $\alpha$ 2 and bind it similarly ( $5.5 \pm 0.9$  ng of arrestin-2 and  $7.7 \pm 1.2$  ng of arrestin-3 detected in one-fifth of eluted samples). These data are the first experimental demonstration that JNK3 $\alpha$ 2 directly binds nonvisual arrestins. This finding raises the question of the affinity of these interactions. This information is critical to understanding the biochemical mechanism of proposed arrestin-mediated scaffolding of MAPK cascades and to evaluating the possible biological role of these processes in cells. We used FRET to determine the dissociation constants ( $K_D$ ) between JNK3 $\alpha$ 2 and the two nonvisual arrestins. Single-cysteine mutants arrestin-2-L101C and arrestin-3-F234C were constructed on the background of fully functional cysteine-less arrestin-2 and -3,<sup>17,30</sup> respectively, and labeled with fluorescein (donor); WT JNK3 $\alpha$ 2 was labeled with Alexa 568 (acceptor) at its natural solvent-exposed cysteines. A His tag pull-down assay was performed to compare the binding abilities of the unlabeled and fluorescently labeled proteins (Figure 2C). The results showed that the addition of fluorescent probes does not significantly perturb the interaction of arrestin with JNK3 $\alpha$ 2 (Figure 2C).

Upon excitation at 485 nm, donor-only samples (50 nM arrestin-2-L101F or arrestin-3-F234F) displayed a single fluorescence peak at 518 nm, while the acceptor-only samples (JNK3 $\alpha$ 2R, 1  $\mu$ M) displayed only a fluorescence peak at 600 nm. The increased amplitude of the fluorescence peak at 600 nm was apparent in samples that contained both donor and acceptor (Figure S1A,B of the Supporting Information). FRET

was observed as both a decrease in the fluorescence of the arrestin-bound donor at 518 nm in the presence of the acceptor and an increase in the fluorescence intensity of the acceptor at 600 nm. FRET titrations were performed via addition of increasing concentrations of JNK3 $\alpha$ 2R, from 0.5 to 10  $\mu$ M, to 50 nM fluorescein-labeled arrestin (Figure 2D,E). The dissociation constants were determined using the decrease in the magnitude of the donor signal upon addition of the acceptor. JNK3 $\alpha$ 2R binds arrestin-2 and arrestin-3 with similar affinities, with  $K_D$  values of  $6.1 \pm 1.8$  and  $4.4 \pm 1.1$   $\mu$ M, respectively (Figure 2F). These data represent the first direct measurement of the affinity of any arrestin for any MAP kinase.

**Biphasic Effect of Arrestin Concentration on JNK3 $\alpha$ 2 Phosphorylation and Activation by MKK4.** Although proteins scaffolding MAP kinase cascades are believed to have profound effects on MAPK signaling, the biochemical mechanism of the function of scaffolds is poorly understood.<sup>31</sup> The biphasic effect of scaffold concentration on MAPK signaling has been predicted by several computational models<sup>23,24,31</sup> and experimentally demonstrated for only Ste5, which scaffolds the Ste4–Ste11–Ste7–Fus3MAPK cascade in yeast in vivo.<sup>32</sup> Figure 3A shows a simplified model illustrating Locasale’s three-state mechanism<sup>24</sup> that explains the biphasic effect of the scaffold. According to this model, JNK3 $\alpha$ 2 can exist in three states: bound to upstream kinase MKK4 in solution, bound to scaffold protein not associated with MKK4 to form an incomplete complex, or bound to scaffold simultaneously with MKK4 in an active signaling complex. An increase in scaffold concentration in the lower range enhances the formation of an active complex containing both kinases, thereby facilitating the activation of the downstream kinase. In contrast, a further increase in scaffold concentration increases the probability of downstream and upstream kinase associating with the scaffold protein alone, forming incomplete inactive complexes. Therefore, the activation of MAPK by its upstream kinase can be inhibited by high concentrations of scaffolds. Kinase suppressor of Ras (KSR), an ERK1/2 cascade scaffold protein, was the first mammalian MAPK scaffold shown to have a biphasic effect on the activation of ERK1/2 and its downstream signaling.<sup>33</sup>

To directly test the mechanism of arrestin action, we used three purified proteins to reconstruct the arrestin-3–MKK4–JNK3 $\alpha$ 2 signaling module. Because arrestin-3 was reported to be phosphorylated by another MAP kinase, ERK2,<sup>34</sup> we first tested whether active MKK4 and/or active JNK3 $\alpha$ 2 can phosphorylate nonvisual arrestins (Figure 3B). We found that neither active MKK4 nor active JNK3 $\alpha$ 2 phosphorylates arrestin-2 or arrestin-3 under our assay conditions. To evaluate the functional role of arrestins, we kept the concentrations of active MKK4 (50 nM) and its substrate, unphosphorylated JNK3 $\alpha$ 2 (0.5  $\mu$ M), constant and measured the extent of phosphorylation of JNK3 $\alpha$ 2 by MKK4 in the presence of various arrestin concentrations (0–30  $\mu$ M). Both nonvisual arrestins demonstrate a bell-shaped concentration dependence of JNK3 $\alpha$ 2 activation by MKK4. JNK3 $\alpha$ 2 phosphorylation was enhanced at low arrestin concentrations but inhibited at higher concentrations. At 5 s, the highest level of JNK3 $\alpha$ 2 phosphorylation was observed in the presence of 0.6  $\mu$ M arrestin-3. The optimal concentration of arrestin-3 at 10 s is higher,  $\sim 1.2$ –3  $\mu$ M. Interestingly, arrestin-2 also promotes phosphorylation of JNK3 $\alpha$ 2 by MKK4 in this in vitro assay but demonstrates higher optimal concentrations at both time points (1.2 and 3–6  $\mu$ M at 5 and 10 s, respectively) (Figure 3C–E).

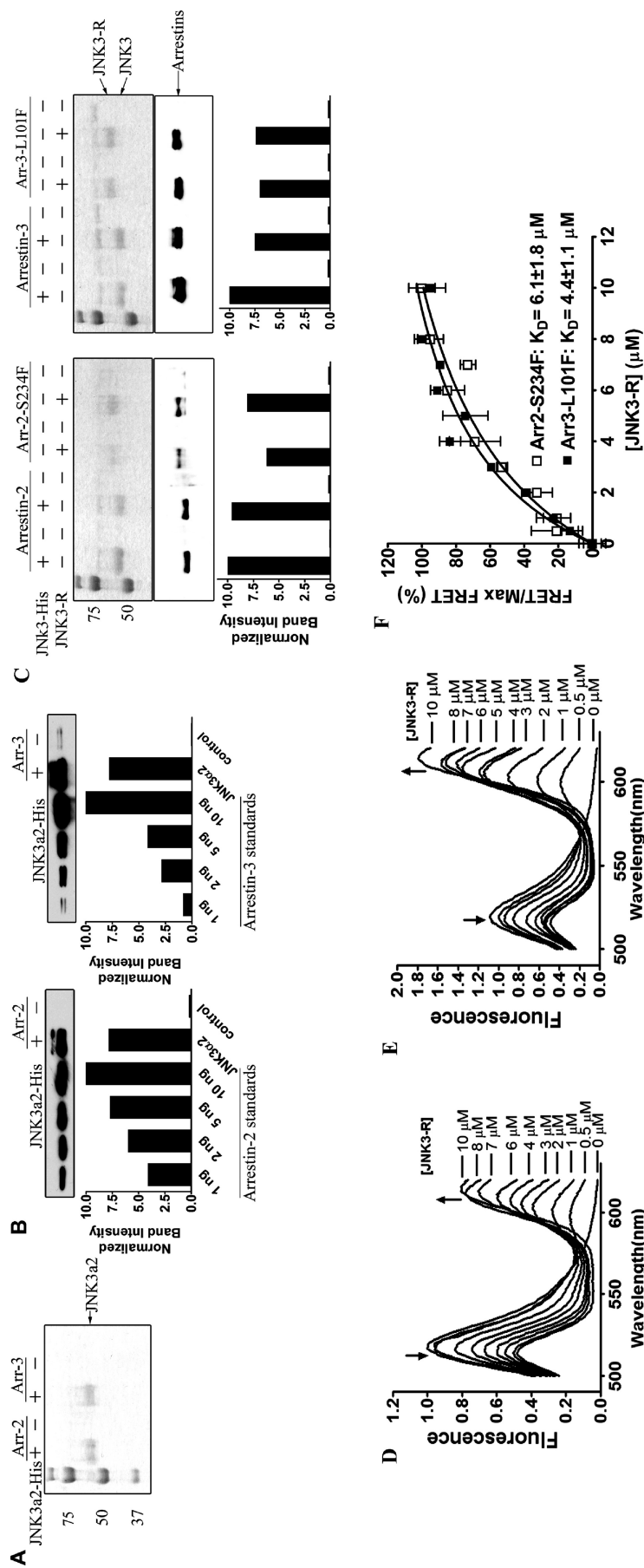


**Figure 2.** Nonvisual arrestins directly bind to JNK3α2 with comparable affinities. (A) Coomassie blue staining of JNK3α2-His eluted from the nickel-NTA column with imidazole, showing equal loading. (B) Western blots of the eluates (one-fifth loaded). Lanes containing known amounts of purified arrestin-2 and -3 standards were used to generate calibration curves. Quantification shows that the JNK3α2-His column retained  $5.5 \pm 0.9$  and  $7.7 \pm 1.2$  ng of arrestin-2 and -3, respectively ( $n = 3$ ). The results demonstrate direct interactions with JNK3α2-His. (C) Fluorescent labeling does not appreciably affect the interaction of arrestin with JNK3α2. JNK3α2-His (JNK3-His) or Alexa 568-labeled JNK3α2-His (JNK3-R, which runs slightly slower on the gel) ( $20 \mu\text{g}$ ) was loaded onto  $50 \mu\text{L}$  of nickel-NTA resin and incubated with purified WT arrestin-2, arrestin-3, or fluorescein-labeled arrestin-2-S234F or arrestin-3-L101F, as indicated. The columns were washed three times with binding buffer, and specifically bound proteins were eluted. One-fifth of each eluate was analyzed by SDS-PAGE: (top) Coomassie blue staining of indicated eluted proteins, (middle) Western blot with a pan-arrestin antibody, and (bottom) quantification of the intensity of arrestin bands. The results of a representative experiment of three performed are shown. (D) FRET between arrestin-2-S234F (donor) and JNK3-R (acceptor). Representative emission spectra from experiments in which arrestin-3-L101F ( $50 \text{ nM}$ ) was incubated with indicated concentrations of JNK3-R ( $0$ – $10 \mu\text{M}$ ) with excitation at  $485 \text{ nm}$ . All spectra were normalized to donor-only fluorescence at  $518 \text{ nm}$ . (E) FRET between arrestin-3-L101F (donor) and JNK3-R (acceptor). Representative emission spectra from experiments in which arrestin-3-L101F ( $50 \text{ nM}$ ) was incubated with the indicated concentrations of JNK3-R ( $0$ – $10 \mu\text{M}$ ) with excitation at  $485 \text{ nm}$ . All spectra are normalized to donor-only fluorescence at  $518 \text{ nm}$ . (F) Binding affinity of nonvisual arrestins for JNK3α2 measured by FRET (D and E). Calculated apparent  $K_D$  values for binding of arrestin-2 and -3 to JNK3α2 were  $6.1 \pm 1.8$  and  $4.4 \pm 1.1 \mu\text{M}$ , respectively ( $n = 3$ ).

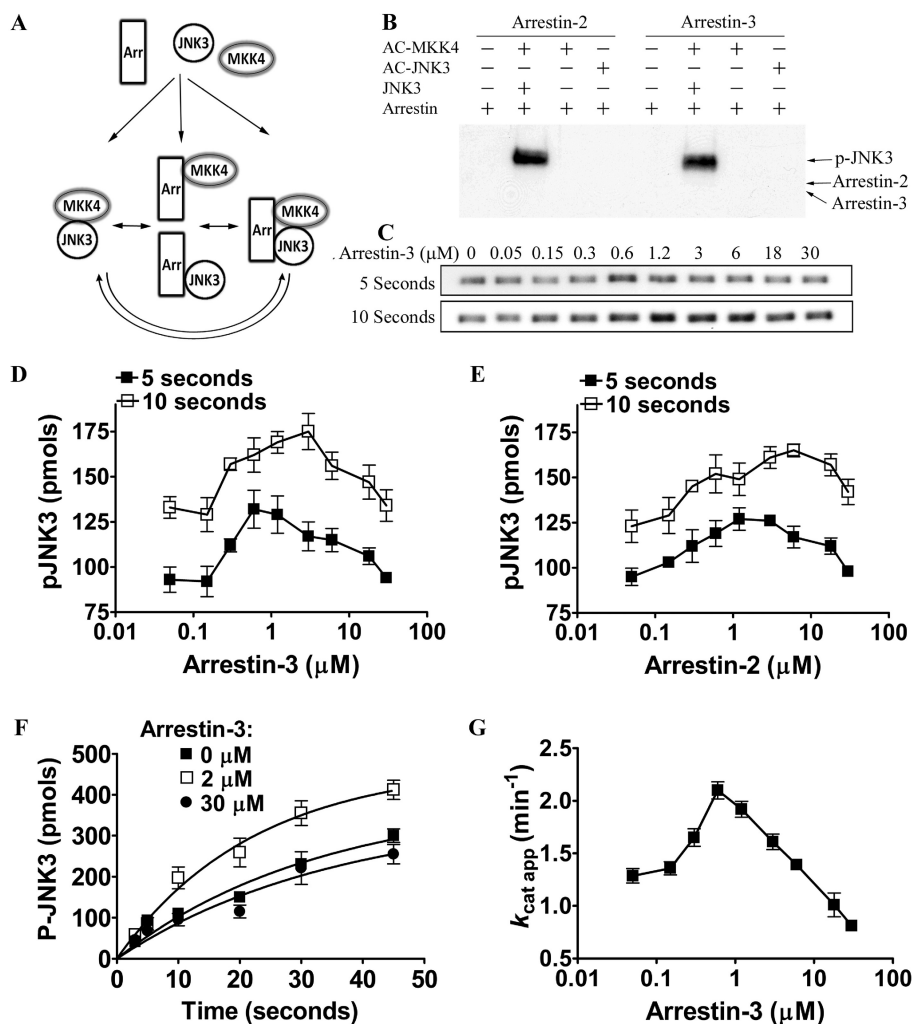


**Figure 3.** Biphasic effects of both nonvisual arrestins on JNK3α2 activation by MKK4. (A) A simplified three-state model showing the scaffolding mechanism of the two-kinase signaling module. A, J, and M stand for arrestin scaffold, JNK3α2, and upstream kinase MKK4, respectively. Kinases can exist in three states: (a) interacting in solution, (b) bound to the scaffold to form incomplete complexes containing a single kinase, and (c) simultaneously tethered by a scaffold to form a complete two-kinase signaling complex. (B) MKK4 and JNK3α2 do not phosphorylate arrestin-2 or -3. Indicated purified arrestins (2 μM) were incubated with active MKK4 (50 nM), active JNK3α2 (50 nM), or inactive JNK3α2 (0.5 μM), as indicated, in kinase buffer for 3 min. The reactions were stopped by 15 μL of SDS sample buffer, and the proteins were separated via 10% SDS-PAGE. The gel was dried and exposed to X-ray film. The autoradiogram from a representative experiment (of three performed) is shown. (C) Representative autoradiograms showing MKK4-phosphorylated JNK3α2 at the indicated concentrations of arrestin-3 at 5 and 10 s. Solutions containing 50 nM active MKK4, 0.5 μM JNK3α2, and 0–30 μM arrestin-3 were premixed and incubated at 30 °C for 15 min. The reactions were initiated by the addition of 0.2 mM ATP (4 μCi of  $\gamma$ - $^{32}$ P) and the mixtures incubated at 30 °C for the indicated time. The reactions were stopped by the addition of Laemmli SDS sample buffer and the mixtures subjected to PAGE on a 10% gel. The autoradiogram from a representative experiment (of three performed) is shown. (D and E) JNK3α2 phosphorylation by MKK4 as a function of arrestin-3 (D) or arrestin-2 (E) concentration at the indicated early time points (5 and 10 s). (F) Time course of JNK3α2 phosphorylation by MKK4 at different arrestin concentrations (0, 2, and 30 μM). (G) ATF2 phosphorylation by JNK3α2 activated by MKK4 at different arrestin-3 concentrations. Solutions containing 50 nM active MKK4, 1 μM JNK3α2, and 0–30 μM arrestin-3 were premixed and incubated at 30 °C for 15 min. The reactions were initiated by the addition of 0.3 mM ATP and the mixtures incubated at 30 °C for 4 min. Seven microliters of the reaction mixture was transferred to another reaction mixture containing 20 μM GST-ATF2 (1–115) and 0.3 mM radiolabeled [ $\gamma$ - $^{32}$ P]ATP (specific activity of  $1 \times 10^{15}$  cpm/mol), yielding a final volume of 70 μL (1:10 dilution). The apparent JNK3α2  $k_{cat}$  was determined and is plotted as a function of arrestin-3 concentration.

Importantly, a biphasic effect of arrestin concentration was also observed by directly measuring the JNK3α2 activity. In these experiments, purified active MKK4 was incubated with JNK3α2 in the presence or absence of arrestin-3, and then the ability of JNK3α2 to phosphorylate its substrate, ATF2, was measured. From these data, the apparent  $k_{cat}$  of JNK3α2 activated by MKK4 at various arrestin-3 concentrations was determined (Figure 3G). These experiments yielded qualitatively similar results: JNK3α2 activation was facilitated by low but inhibited at higher arrestin-3 concentrations, yielding a bell-shaped

concentration dependence, with the highest JNK3α2 activity observed in the presence of 0.6 μM arrestin-3 (Figure 3G), in excellent agreement with JNK3α2 phosphorylation data (Figure 3F).

These findings are consistent with our direct binding data. The biphasic effect would be observed only when scaffolding protein binds both kinases (Figure 3A). Higher optimal concentrations of arrestin-2 (Figure 3E) are consistent with its significantly lower affinity for MKK4 (Figure 1C). In addition to affinities of binary interactions, optimal scaffold



concentrations can also be determined by positive or negative cooperativity of the simultaneous binding of the two kinases to the scaffolding protein.<sup>31</sup> To further explore the underlying mechanisms, we analyzed the time course of JNK3 $\alpha$ 2 activation at different arrestin-3 concentrations (0, 2, and 30  $\mu$ M). In the presence of 2  $\mu$ M arrestin-3, the initial rate of JNK3 $\alpha$ 2 activation by MKK4 (determined in the first 10 s) was increased from  $12.63 \pm 2.1$  to  $19.2 \pm 0.7$  pmol/s, while at 30  $\mu$ M arrestin-3, the initial rate was as low as that in its absence,  $10.7 \pm 1.4$  pmol/s.

## DISCUSSION

Although arrestin-3-dependent JNK3 $\alpha$ 2 activation was reported more than a decade ago,<sup>9</sup> direct interaction of any of the kinases in the ASK1–MKK4–JNK3 $\alpha$ 2 cascade with arrestin-3 has never been demonstrated. In fact, the authors of the two initial studies hypothesized that ASK1 and JNK3 $\alpha$ 2 bind arrestin-3, whereas MKK4 does not,<sup>9,19</sup> and argued that arrestin-2 does not promote JNK3 $\alpha$ 2 activation because, in contrast to arrestin-3, it fails to bind this kinase.<sup>19</sup> Subsequent work suggested that both nonvisual arrestins comparably bind JNK3 $\alpha$ 2,<sup>13,14,18</sup> MKK4,<sup>15</sup> and ASK1;<sup>15</sup> i.e., the binding, per se, does not account for the functional differences between arrestin-2 and -3.<sup>15,18</sup> While the first report suggested that only receptor-associated arrestin-3 facilitates JNK3 $\alpha$ 2 phosphorylation,<sup>9</sup> a subsequent study by the same group showed that free arrestin-3 can also accomplish this.<sup>19</sup> The latter finding was confirmed using WT arrestin-3, as well as an arrestin-3 mutant impaired with respect to receptor binding.<sup>15</sup>

Arrestin-3 was termed a scaffold from the very beginning,<sup>9</sup> even though all previous studies used exclusively cell-based assays and presented no evidence of direct interaction of any of the MAP kinases with arrestin-3.<sup>12–15,19,29</sup> Here we used purified proteins and several interaction assays to show for the first time that both JNK3 $\alpha$ 2 and MKK4 directly bind free arrestin-2 and arrestin-3 (Figures 1B,C and 2). More than 100 nonreceptor partners were reported to bind arrestin-2 and -3.<sup>35</sup> However, very few of these interactions were shown to be direct, as co-IP, with or without subsequent proteomics analysis, used in most studies<sup>9,10,15,19,35</sup> shows that the proteins are in complexes that include arrestins but cannot prove that any of them bind arrestins directly, rather than via another protein serving as an intermediary or scaffold. Considering the recent keen interest in arrestin-mediated signaling (reviewed in refs 8 and 36), direct interaction with arrestins was demonstrated for surprisingly few nonreceptor partners: clathrin,<sup>5,37,38</sup> N-ethylmaleimide-sensitive fusion protein,<sup>39</sup> PDE4D,<sup>40</sup> microtubules,<sup>30,41–43</sup> calmodulin,<sup>16</sup> MEK1,<sup>44</sup> and ubiquitin ligases AIP4<sup>45</sup> and parkin.<sup>17</sup> Various protein kinases were reported to interact with arrestins (reviewed in refs 7 and 8), but JNK3 $\alpha$ 2 and MKK4 are the first for which direct binding has been demonstrated (Figures 1B,C and 2). We also measured the affinity of interactions of JNK3 $\alpha$ 2 with nonvisual arrestins (Figure 2D–F). When typical rate constants for protein–protein interactions are taken into account,<sup>46,47</sup> a  $K_D$  of 4–6  $\mu$ M translates into a half-life of 0.12–0.17 s, which suggests that MAPK complexes with arrestins in cells are fairly transient, as could be expected to support rapid signaling events. Estimated arrestin-2 and -3 concentrations in neurons are submicromolar.<sup>48</sup> Therefore, a low micromolar affinity of JNK3 $\alpha$ 2 means that only a fraction of arrestins at any given moment exists in complex with this kinase in the cell. This is consistent with the notion that arrestins, which are too

small to accommodate more than three or four proteins simultaneously,<sup>1</sup> interact with multiple binding partners,<sup>7,35</sup> so that in the cell each partner associates with a small fraction of the arrestins present. Interestingly, basal expression of Ste5 scaffold in yeast is much lower than necessary for maximal Fus3 activation, which likely allows for the regulation of signaling via changes of Ste5 expression in either direction.<sup>32</sup> Similarly, the level of arrestin-3 in cells<sup>48,49</sup> appears to be suboptimal for the scaffolding of the ASK1–MKK4–JNK3 cascade, possibly for the same reason.

Importantly, our experiments with the arrestin-3–MKK4–JNK3 $\alpha$ 2 complex reconstructed from purified proteins show that the ratio of the scaffold and the two kinases determines the time course of the signaling (Figure 3). These data provide the first experimental support for the theoretical model proposed previously.<sup>31</sup> These results suggest that the relatively low level of expression of arrestin-3 in mature neurons<sup>48,49</sup> ensures rapid and transient JNK3 $\alpha$ 2 activation, which makes perfect biological sense in these irreplaceable postmitotic cells. Arrestin-2 binds JNK3 $\alpha$ 2 and MKK4 (Figures 1C and 2B) but does not activate JNK3 $\alpha$ 2 in cells,<sup>15,19</sup> suggesting that it acts in a dominant-negative fashion, suppressing JNK3 $\alpha$ 2 activity, thereby likely promoting cell survival. This is consistent with roughly equal expression of arrestin-2 and -3 in neuronal precursors,<sup>49</sup> which is converted into a large 10–20-fold excess of arrestin-2 over arrestin-3 by means of a rapid increase in the level of arrestin-2 expression as neurons mature.<sup>48,49</sup>

While the idea that free arrestin-3 can promote JNK3 $\alpha$ 2 activation was proposed previously,<sup>15,19</sup> our data provide the first unambiguous evidence that this is the case (Figure 3). Interestingly, our data suggest that quantitative differences in the affinity of arrestin-2 and -3 for these kinases translate into a qualitative difference between lack of activity and effective JNK3 $\alpha$ 2 activation in the cell, where the levels of arrestins, MKK4, and JNK3 $\alpha$ 2 are relatively low and tightly regulated. Obviously, we cannot exclude the possibility that this difference is partially due to differential ASK1 binding, although indirect evidence based on co-IP suggests that this is unlikely.<sup>15,18</sup> This issue can be definitively resolved only by the reconstruction from pure proteins of the complete ASK1–MKK4–JNK3 $\alpha$ 2 signaling module with arrestin-2 and -3.

Arrestins in the cell exist in at least three distinct conformations: (1) free, closely resembling crystal structures,<sup>27,50–53</sup> (2) receptor-bound, and (3) microtubule-bound (reviewed in ref 54). The proteins that engage the well-defined receptor-binding surface<sup>25,55–60</sup> do not interact with receptor-associated arrestins.<sup>16,42,61,62</sup> The partners whose interaction sites do not overlap with that of GPCRs show distinct conformational preferences: ERK2 appears to prefer receptor-bound arrestin,<sup>15,26</sup> ubiquitin ligases Mdm2 and parkin preferentially interact with arrestins in the basal conformation,<sup>14,15,17,29</sup> whereas JNK3 $\alpha$ 2 does not seem to care one way or the other.<sup>14,15,29</sup> We demonstrated that free arrestin-3 at its optimal concentration promotes phosphorylation of JNK3 $\alpha$ 2 by MKK4. However, only direct kinetic comparison of this complex with the one similarly reconstructed from pure proteins containing receptor-associated arrestin-3 can definitively show whether receptor binding plays any role in this signaling other than simply concentrating the arrestins and associated kinases in the vicinity of receptor-rich membranes.

In conclusion, the first reconstruction from pure proteins of the signaling complex organized by arrestin revealed that both MKK4 and JNK3 $\alpha$ 2 directly bind free arrestin-3, which acts as a

true scaffold facilitating phosphorylation of JNK3 $\alpha$ 2 by MKK4 simply by simultaneously binding these two kinases, bringing them into the proximity of each other. This work demonstrates that experiments with pure proteins in strictly controlled conditions can yield definitive answers that remained elusive when only cell-based assays were in use. Further experimentation with pure proteins is necessary to reveal possible differences in MAPK scaffolding by free and receptor-bound arrestins, which is necessary for the elucidation of the biological role of these events in cell signaling, as well as for devising ways of targeting this process for therapeutic purposes.

## ■ ASSOCIATED CONTENT

### ● Supporting Information

FRET between fluorescently labeled arrestin-2 and -3 and JNK3 (Figure S1). This material is available free of charge via the Internet at <http://pubs.acs.org>.

## ■ AUTHOR INFORMATION

### Corresponding Author

\*Department of Pharmacology, Vanderbilt University, Nashville, TN 37232. Telephone: (615) 322-7070. E-mail: [vsevolod.gurevich@vanderbilt.edu](mailto:vsevolod.gurevich@vanderbilt.edu).

### Funding

Supported by National Institutes of Health Grants GM077561, GM081756, EY011500 (V.V.G.), and GM059802 and Welch Foundation Grant F-1390 (K.N.D.).

## ■ ABBREVIATIONS

GPCR, G protein-coupled receptor; MAPK or MAP kinase, mitogen-activated protein kinase; JNK3 $\alpha$ 2, c-Jun N-terminal kinase 3 $\alpha$ 2; MKK4, MAP kinase kinase 4; ERK1/2, extracellular signal-regulated kinase 1/2; GRK, G protein-coupled receptor kinase; GST, glutathione S-transferase; LB, Luria Broth; PMSF, phenylmethanesulfonyl fluoride; FRET, fluorescence resonance energy transfer.

## ■ ADDITIONAL NOTE

<sup>a</sup>We use systematic names of arrestin proteins: arrestin-1 (historic names S-antigen, 48 kDa protein, or visual or rod arrestin), arrestin-2 (b-arrestin or b-arrestin1), arrestin-3 (b-arrestin2 or hTHY-ARRX), and arrestin-4 (cone or X-arrestin; for unclear reasons, its gene is called *arrestin 3* in the HUGO database).

## ■ REFERENCES

- (1) Gurevich, V. V., and Gurevich, E. V. (2006) The structural basis of arrestin-mediated regulation of G protein-coupled receptors. *Pharm. Ther.* 110, 465–502.
- (2) Gurevich, V. V., Hanson, S. M., Song, X., Vishnivetskiy, S. A., and Gurevich, E. V. (2011) The functional cycle of visual arrestins in photoreceptor cells. *Prog. Retinal Eye Res.* 30, 405–430.
- (3) Krupnick, J. G., Gurevich, V. V., and Benovic, J. L. (1997) Mechanism of quenching of phototransduction. Binding competition between arrestin and transducin for phosphorhodopsin. *J. Biol. Chem.* 272, 18125–18131.
- (4) Wilden, U. (1995) Duration and amplitude of the light-induced cGMP hydrolysis in vertebrate photoreceptors are regulated by multiple phosphorylation of rhodopsin and by arrestin binding. *Biochemistry* 34, 1446–1454.
- (5) Goodman, O. B. Jr., Krupnick, J. G., Santini, F., Gurevich, V. V., Penn, R. B., Gagnon, A. W., Keen, J. H., and Benovic, J. L. (1996)  $\beta$ -Arrestin acts as a clathrin adaptor in endocytosis of the  $\beta$ 2-adrenergic receptor. *Nature* 383, 447–450.
- (6) Laporte, S. A., Oakley, R. H., Zhang, J., Holt, J. A., Ferguson, S. S., Caron, M. G., and Barak, L. S. (1999) The  $\beta$ 2-adrenergic receptor/arrestin complex recruits the clathrin adaptor AP-2 during endocytosis. *Proc. Natl. Acad. Sci. U.S.A.* 96, 3712–3717.
- (7) Gurevich, E. V., and Gurevich, V. V. (2006) Arrestins are ubiquitous regulators of cellular signaling pathways. *Genome Biol.* 7, 236.
- (8) DeWire, S. M., Ahn, S., Lefkowitz, R. J., and Shenoy, S. K. (2007)  $\beta$ -Arrestins and cell signaling. *Annu. Rev. Physiol.* 69, 483–510.
- (9) McDonald, P. H., Chow, C. W., Miller, W. E., Laporte, S. A., Field, M. E., Lin, F. T., Davis, R. J., and Lefkowitz, R. J. (2000)  $\beta$ -Arrestin 2: A receptor-regulated MAPK scaffold for the activation of JNK3. *Science* 290, 1574–1577.
- (10) Luttrell, L. M., Roudabush, F. L., Choy, E. W., Miller, W. E., Field, M. E., Pierce, K. L., and Lefkowitz, R. J. (2001) Activation and targeting of extracellular signal-regulated kinases by  $\beta$ -arrestin scaffolds. *Proc. Natl. Acad. Sci. U.S.A.* 98, 2449–2454.
- (11) Bruchas, M. R., Macey, T. A., Lowe, J. D., and Chavkin, C. (2006) Kappa opioid receptor activation of p38 MAPK is GRK3- and arrestin-dependent in neurons and astrocytes. *J. Biol. Chem.* 281, 18081–18089.
- (12) Scott, M. G., Le Rouzic, E., Perianin, A., Pierotti, V., Enslin, H., Benichou, S., Marullo, S., and Benmerah, A. (2002) Differential nucleocytoplasmic shuttling of  $\beta$ -arrestins. Characterization of a leucine-rich nuclear export signal in  $\beta$ -arrestin2. *J. Biol. Chem.* 277, 37693–37701.
- (13) Wang, P., Wu, Y., Ge, X., Ma, L., and Pei, G. (2003) Subcellular localization of  $\beta$ -arrestins is determined by their intact N domain and the nuclear export signal at the C terminus. *J. Biol. Chem.* 278, 11648–11653.
- (14) Song, X., Raman, D., Gurevich, E. V., Vishnivetskiy, S. A., and Gurevich, V. V. (2006) Visual and both non-visual arrestins in their “inactive” conformation bind JNK3 and Mdm2 and relocate them from the nucleus to the cytoplasm. *J. Biol. Chem.* 281, 21491–21499.
- (15) Song, X., Coffa, S., Fu, H., and Gurevich, V. V. (2009) How does arrestin assemble MAPKs into a signaling complex? *J. Biol. Chem.* 284, 685–695.
- (16) Wu, N., Hanson, S. M., Francis, D. J., Vishnivetskiy, S. A., Thibonnier, M., Klug, C. S., Shoham, M., and Gurevich, V. V. (2006) Arrestin binding to calmodulin: A direct interaction between two ubiquitous signaling proteins. *J. Mol. Biol.* 364, 955–963.
- (17) Ahmed, M. R., Zhan, X., Song, X., Kook, S., Gurevich, V. V., and Gurevich, E. V. (2011) Ubiquitin ligase parkin promotes Mdm2-arrestin interaction but inhibits arrestin ubiquitination. *Biochemistry* 50, 3749–3763.
- (18) Seo, J., Tsakem, E. L., Breitman, M., and Gurevich, V. V. (2011) Identification of arrestin-3-specific residues necessary for JNK3 activation. *J. Biol. Chem.* 286, 27894–27901.
- (19) Miller, W. E., McDonald, P. H., Cai, S. F., Field, M. E., Davis, R. J., and Lefkowitz, R. J. (2001) Identification of a motif in the carboxyl terminus of  $\beta$ -arrestin2 responsible for activation of JNK3. *J. Biol. Chem.* 276, 27770–27777.
- (20) Dhanasekaran, D. N., Kashef, K., Lee, C. M., Xu, H., and Reddy, E. P. (2007) Scaffold proteins of MAP-kinase modules. *Oncogene* 26, 3185–3202.
- (21) Yoshioka, K. (2004) Scaffold Proteins in Mammalian MAP Kinase Cascades. *J. Biochem.* 135, 657–661.
- (22) Dard, N., and Peter, M. (2006) Scaffold proteins in MAP kinase signaling: More than simple passive activating platforms. *BioEssays* 28, 146–156.
- (23) Locasale, J. W., and Chakraborty, A. K. (2008) Regulation of signal duration and the statistical dynamics of kinase activation by scaffold proteins. *PLoS Comput. Biol.* 4, e1000099.
- (24) Locasale, J. W. (2008) Three-state kinetic mechanism for scaffold-mediated signal transduction. *Phys. Rev. E: Stat., Nonlinear, Soft Matter* 78, 051921.
- (25) Vishnivetskiy, S. A., Gimenez, L. E., Francis, D. J., Hanson, S. M., Hubbell, W. L., Klug, C. S., and Gurevich, V. V. (2011) Few residues within an extensive binding interface drive receptor



interaction and determine the specificity of arrestin proteins. *J. Biol. Chem.* 286, 24288–24299.

(26) Coffa, S., Breitman, M., Spiller, B. W., and Gurevich, V. V. (2011) A single mutation in arrestin-2 prevents ERK1/2 activation by reducing c-Raf1 binding. *Biochemistry* 50, 6951–6958.

(27) Zhan, X., Gimenez, L. E., Gurevich, V. V., and Spiller, B. W. (2011) Crystal structure of arrestin-3 reveals the basis of the difference in receptor binding between two non-visual arrestins. *J. Mol. Biol.* 406, 467–478.

(28) Gurevich, V. V., and Benovic, J. L. (2000) Arrestin: Mutagenesis, expression, purification, and functional characterization. *Methods Enzymol.* 315, 422–437.

(29) Song, X., Gurevich, E. V., and Gurevich, V. V. (2007) Cone arrestin binding to JNK3 and Mdm2: Conformational preference and localization of interaction sites. *J. Neurochem.* 103, 1053–1062.

(30) Hanson, S. M., Cleghorn, W. M., Francis, D. J., Vishnivetskiy, S. A., Raman, D., Song, X., Nair, K. S., Slepak, V. Z., Klug, C. S., and Gurevich, V. V. (2007) Arrestin mobilizes signaling proteins to the cytoskeleton and redirects their activity. *J. Mol. Biol.* 368, 375–387.

(31) Levchenko, A., Bruck, J., and Sternberg, P. W. (2000) Scaffold proteins may biphasically affect the levels of mitogen-activated protein kinase signaling and reduce its threshold properties. *Proc. Natl. Acad. Sci. U.S.A.* 97, 5818–5823.

(32) Chapman, S. A., and Asthagiri, A. R. (2009) Quantitative effect of scaffold abundance on signal propagation. *Mol. Syst. Biol.* 5, 313.

(33) Kortum, R. L., and Lewis, R. E. (2004) The molecular scaffold KSR1 regulates the proliferative and oncogenic potential of cells. *Mol. Cell. Biol.* 24, 4407–4416.

(34) Lin, F. T., Miller, W. E., Luttrell, L. M., and Lefkowitz, R. J. (1999) Feedback regulation of  $\beta$ -arrestin1 function by extracellular signal-regulated kinases. *J. Biol. Chem.* 274, 15971–15974.

(35) Xiao, K., McClatchy, D. B., Shukla, A. K., Zhao, Y., Chen, M., Shenoy, S. K., Yates, J. R., and Lefkowitz, R. J. (2007) Functional specialization of  $\beta$ -arrestin interactions revealed by proteomic analysis. *Proc. Natl. Acad. Sci. U.S.A.* 104, 12011–12016.

(36) Gurevich, V. V., and Gurevich, E. V. (2010) Custom-designed proteins as novel therapeutic tools? The case of arrestins. *Expert Rev. Mol. Med.* 12, e13.

(37) Krupnick, J. G., Goodman, O. B. Jr., Keen, J. H., and Benovic, J. L. (1997) Arrestin/clathrin interaction. Localization of the clathrin binding domain of nonvisual arrestins to the carboxy terminus. *J. Biol. Chem.* 272, 15011–15016.

(38) Goodman, O. B. Jr., Krupnick, J. G., Gurevich, V. V., Benovic, J. L., and Keen, J. H. (1997) Arrestin/clathrin interaction. Localization of the arrestin binding locus to the clathrin terminal domain. *J. Biol. Chem.* 272, 15017–15022.

(39) McDonald, P. H., Cote, N. L., Lin, F. T., Premont, R. T., Pitcher, J. A., and Lefkowitz, R. J. (1999) Identification of NSF as a  $\beta$ -arrestin1-binding protein. Implications for  $\beta$ 2-adrenergic receptor regulation. *J. Biol. Chem.* 274, 10677–10680.

(40) Baillie, G. S., Adams, D. R., Bhari, N., Houslay, T. M., Vadrevu, S., Meng, D., Li, X., Dunlop, A., Milligan, G., Bolger, G. B., Klusmann, E., and Houslay, M. D. (2007) Mapping binding sites for the PDE4D5 cAMP-specific phosphodiesterase to the N- and C-domains of  $\beta$ -arrestin using spot-immobilized peptide arrays. *Biochem. J.* 404, 71–80.

(41) Nair, K. S., Hanson, S. M., Kennedy, M. J., Hurley, J. B., Gurevich, V. V., and Slepak, V. Z. (2004) Direct binding of visual arrestin to microtubules determines the differential subcellular localization of its splice variants in rod photoreceptors. *J. Biol. Chem.* 279, 41240–41248.

(42) Nair, K. S., Hanson, S. M., Mendez, A., Gurevich, E. V., Kennedy, M. J., Shestopalov, V. I., Vishnivetskiy, S. A., Chen, J., Hurley, J. B., Gurevich, V. V., and Slepak, V. Z. (2005) Light-dependent redistribution of arrestin in vertebrate rods is an energy-independent process governed by protein-protein interactions. *Neuron* 46, 555–567.

(43) Hanson, S. M., Francis, D. J., Vishnivetskiy, S. A., Klug, C. S., and Gurevich, V. V. (2006) Visual arrestin binding to microtubules

involves a distinct conformational change. *J. Biol. Chem.* 281, 9765–9772.

(44) Meng, D., Lynch, M. J., Huston, E., Beyermann, M., Eichhorst, J., Adams, D. R., Klusmann, E., Houslay, M. D., and Baillie, G. S. (2009) MEK1 binds directly to  $\beta$ arrestin1, influencing both its phosphorylation by ERK and the timing of its isoprenaline-stimulated internalization. *J. Biol. Chem.* 284, 11425–11435.

(45) Bhandari, D., Trejo, J., Benovic, J. L., and Marchese, A. (2007) Arrestin-2 interacts with the ubiquitin-protein isopeptide ligase atrophin-interacting protein 4 and mediates endosomal sorting of the chemokine receptor CXCR4. *J. Biol. Chem.* 282, 36971–36979.

(46) Northrup, S. H., and Erickson, H. P. (1992) Kinetics of protein-protein association explained by Brownian dynamics computer simulation. *Proc. Natl. Acad. Sci. U.S.A.* 89, 3338–3342.

(47) Bayburt, T. H., Vishnivetskiy, S. A., McLean, M., Morizumi, T., Huang, C.-c., Tesmer, J. J., Ernst, O. P., Sligar, S. G., and Gurevich, V. V. (2011) Rhodopsin monomer is sufficient for normal rhodopsin kinase (GRK1) phosphorylation and arrestin-1 binding. *J. Biol. Chem.* 286, 1420–1428.

(48) Gurevich, E. V., Benovic, J. L., and Gurevich, V. V. (2004) Arrestin2 expression selectively increases during neural differentiation. *J. Neurochem.* 91, 1404–1416.

(49) Gurevich, E. V., Benovic, J. L., and Gurevich, V. V. (2002) Arrestin2 and arrestin3 are differentially expressed in the rat brain during postnatal development. *Neuroscience* 109, 421–436.

(50) Hirsch, J. A., Schubert, C., Gurevich, V. V., and Sigler, P. B. (1999) The 2.8 Å crystal structure of visual arrestin: A model for arrestin's regulation. *Cell* 97, 257–269.

(51) Han, M., Gurevich, V. V., Vishnivetskiy, S. A., Sigler, P. B., and Schubert, C. (2001) Crystal structure of  $\beta$ -arrestin at 1.9 Å: Possible mechanism of receptor binding and membrane translocation. *Structure* 9, 869–880.

(52) Milano, S. K., Pace, H. C., Kim, Y. M., Brenner, C., and Benovic, J. L. (2002) Scaffolding functions of arrestin-2 revealed by crystal structure and mutagenesis. *Biochemistry* 41, 3321–3328.

(53) Sutton, R. B., Vishnivetskiy, S. A., Robert, J., Hanson, S. M., Raman, D., Knox, B. E., Kono, M., Navarro, J., and Gurevich, V. V. (2005) Crystal Structure of Cone Arrestin at 2.3 Å: Evolution of Receptor Specificity. *J. Mol. Biol.* 354, 1069–1080.

(54) Gurevich, V. V., Gurevich, E. V., and Cleghorn, W. M. (2008) Arrestins as multi-functional signaling adaptors. *Handb. Exp. Pharmacol.* 186, 15–37.

(55) Ohguro, H., Palczewski, K., Walsh, K. A., and Johnson, R. S. (1994) Topographic study of arrestin using differential chemical modifications and hydrogen/deuterium exchange. *Protein Sci.* 3, 2428–2434.

(56) Pulvermuller, A., Schroder, K., Fischer, T., and Hofmann, K. P. (2000) Interactions of metarhodopsin II. Arrestin peptides compete with arrestin and transducin. *J. Biol. Chem.* 275, 37679–37685.

(57) Gurevich, V. V., and Benovic, J. L. (1995) Visual arrestin binding to rhodopsin: Diverse functional roles of positively charged residues within the phosphorylation-recognition region of arrestin. *J. Biol. Chem.* 270, 6010–6016.

(58) Vishnivetskiy, S. A., Hosey, M. M., Benovic, J. L., and Gurevich, V. V. (2004) Mapping the arrestin-receptor interface: Structural elements responsible for receptor specificity of arrestin proteins. *J. Biol. Chem.* 279, 1262–1268.

(59) Hanson, S. M., and Gurevich, V. V. (2006) The differential engagement of arrestin surface charges by the various functional forms of the receptor. *J. Biol. Chem.* 281, 3458–3462.

(60) Hanson, S. M., Francis, D. J., Vishnivetskiy, S. A., Kolobova, E. A., Hubbell, W. L., Klug, C. S., and Gurevich, V. V. (2006) Differential interaction of spin-labeled arrestin with inactive and active phosphorhodopsin. *Proc. Natl. Acad. Sci. U.S.A.* 103, 4900–4905.

(61) Hanson, S. M., Van Eps, N., Francis, D. J., Altenbach, C., Vishnivetskiy, S. A., Arshavsky, V. Y., Klug, C. S., Hubbell, W. L., and Gurevich, V. V. (2007) Structure and function of the visual arrestin oligomer. *EMBO J.* 26, 1726–1736.

(62) Hanson, S. M., Dawson, E. S., Francis, D. J., Van Eps, N., Klug, C. S., Hubbell, W. L., Meiler, J., and Gurevich, V. V. (2008) A model for the solution structure of the rod arrestin tetramer. *Structure* 16, 924–934.